# Interdomain wall in amorphous glass-coated microwires

H. Chiriac, T.-A. Óvári, S. Corodeanu, and G. Ababei
*National Institute of Research and Development for Technical Physics, 47 Mangeron Boulevard, RO-700050 Iaşi, Romania*
(Received 13 July 2007; revised manuscript received 17 September 2007; published 27 December 2007)

Amorphous glass-coated microwires display a core-shell-type magnetic structure, whose main components, the inner core and the outer shell, have been extensively studied. In this paper, the interdomain wall that separates these two main components of the core-shell structure is investigated. The wall position and width in microwires with various compositions and dimensions are calculated. Experimental investigation techniques, such as ferromagnetic resonance, ultrahigh frequency giant magnetoimpedance, and axial hysteresis loop measurements, are subsequently employed to investigate those regions of the microwires in which the presence of the interdomain wall is expected to have the most significant effects. The investigation of the interdomain wall unveils aspects of the magnetism of these materials and opens up the way for the development of methods of controlled optimization of their magnetic properties in order to improve their response as sensitive elements in magnetic sensor devices.

DOI: 10.1103/PhysRevB.76.214433 PACS number(s): 75.50.Kj, 75.60.Ch, 75.70.Rf

## I. INTRODUCTION

Presently, there is a major worldwide interest in amorphous magnetic materials with excellent soft magnetic properties, since they are appropriate both for studies of fundamental magnetism,[1] as well as for applications in magnetic sensors with high sensitivity and for the miniaturization of existing sensor devices employing polycrystalline materials as sensing elements.[2]

Materials with cylindrical symmetry are an important category within the class of amorphous magnetic materials, amorphous magnetic wires, and glass-coated microwires being the most typical examples of such materials. Both wires and microwires produced by rapid solidification from the melt are suitable candidates for various sensor applications.[3] Among them, amorphous glass-coated microwires with diameters of the metallic nucleus, $D_m$, between 1 and 40 $\mu$m and the glass coating thickness, $t_g$, between 1 and 30 $\mu$m display a unique magnetic behavior, which is suitable for applications in magnetic sensor devices operating on principles such as the giant magnetoimpedance (GMI) effect, the large Barkhausen effect (LBE), and the Matteucci or inverse Wiedemann effects.[4–6] The appearance of these effects is the result of their unique magnetic domain structure, whose formation is determined by the coupling between magnetostriction and the large internal stresses induced during preparation.[7,8] Thus, the sign and magnitude of the magnetostriction constant are, besides the sign, the magnitude, and the orientation of induced internal stresses, the key parameters that allow one to understand the magnetic phenomena which take place in these materials.

Because of the absence of the long range ordering of ions, amorphous microwires do not display magnetocrystalline anisotropy, and the magnetoelastic anisotropy originating in the coupling between internal stresses and magnetostriction plays the essential role in their magnetization process. The formation of the domain structure and the distribution of the magnetoelastic anisotropy axes in glass-coated amorphous microwires result mainly from the minimization of the magnetoelastic energy term, which is the preponderant term in their total free energy.

The domain structure of amorphous microwires typically consists of an inner core (IC) and an outer shell (OS) with various orientations of their easy axes of magnetization. For instance, in amorphous microwires with positive magnetostriction, e.g., $Fe_{77.5}Si_{7.5}B_{15}$ with the saturation magnetostriction constant $\lambda_S = 25 \times 10^{-6}$, the IC is always axially magnetized while the OS displays a radial easy axis of magnetization. This domain structure, together with the fact that the IC occupies most of the volume of the microwire's metallic nucleus, leads to an axial magnetization process that takes place through a single and large jump of the magnetization, i.e., through an LBE.[9] In amorphous microwires with negative magnetostriction, e.g., $Co_{80}Si_{10}B_{10}$ with $\lambda_S = -4 \times 10^{-6}$, both the IC and the OS display transverse easy axes of magnetization, resulting in an almost anhysteretic *BH* loop.[10] It has been recently shown[11] that as-cast glass-coated amorphous microwires with nearly zero magnetostriction, e.g., $Co_{68.15}Fe_{4.35}Si_{12.5}B_{15}$ with $\lambda_S = -1 \times 10^{-7}$, display two types of *BH* loops, depending on their dimensions: for metallic core diameters smaller than 20 $\mu$m their *BH* loop looks similar to that of negative magnetostrictive microwires, i.e., almost anhysteretic, whereas if the metallic core diameter exceeds 20 $\mu$m, they display a *BH* loop typical for a sample which is magnetized through LBE. This change in the mechanism of magnetization is associated with the very fine balance between the magnetoelastic and magnetostatic energy terms in these microwires with small and negative magnetostriction. While their OS is always circumferentially magnetized, the orientation of the easy axis within the IC depends on whether the magnetoelastic or the magnetostatic term is larger, having a transverse orientation for a preponderant magnetoelastic term and an axial one for a preponderant magnetostatic term.

The main elements of the domain structure of amorphous microwires have been analyzed and discussed by many authors from the research groups focused on the investigation of these materials. These elements include the IC and the OS,[12–14] as well as the 180° domain wall which propagates within the IC of microwires displaying LBE, and which separates the IC from the end domains with reversed magnetization that appear in order to diminish the overall magne-

 

tostatic energy.[15,16] Almost any report dealing with amorphous microwires refers to the IC and the OS. The IC is mostly referred to in reports dealing with the axial magnetization process and low frequency phenomena, while the OS is the main topic of investigation in reports dealing with high frequency phenomena such as the GMI effect or ferromagnetic resonance (FMR), due to the skin effect that appears at high frequencies.[17]

Even though this simple representation of the domain structure of microwires is able to explain many peculiarities of their magnetic behavior, it certainly does not stand for their entire domain structure. In support for this statement we bring experimental results that cannot be explained based only on the present knowledge of the domain structure. One such result is the dependence of the GMI effect on microwire dimensions in the case of microwires with the diameter of their metallic nucleus below 10 $\mu$m, in which the magnitude of the GMI effect in some cases increases instead of decreasing as predicted by the known domain structure and anisotropy distribution.[18] Another result which seems at least contradictory if analyzed only based on the current knowledge of the domain structure refers to the magneto-optical Kerr effect studies performed on microwires with nearly zero magnetostriction, and which show that in such microwires with very thin glass coating, the direction of the easy axis in their surface region is helical.[19] Such an unusual result basically contradicts the tensor character of internal stresses by allowing a smaller nondiagonal stress component, rather than a dominant diagonal one, to couple with magnetostriction and decide the anisotropy direction.

The investigation of an important element of the core-shell domain structure, which has been omitted in the previous studies performed on amorphous microwires, is expected to explain the above mentioned intriguing results and, at the same time, to open up opportunities in the basic research of amorphous magnetic microwires as well as in their applications in magnetic sensor devices. This important element of the domain structure is the interdomain wall that separates the main regions of the domain structure, i.e., the interdomain wall (IDW) between the IC and the OS.

The aim of this paper is to investigate this important element of the magnetic structure of amorphous ferromagnets with cylindrical symmetry. We have studied separately the cases of positive, negative, and nearly zero magnetostrictive microwires, since it is expected to have different characteristics and effects of the IDW in materials with different signs and magnitudes of the magnetostriction constant. We have focused on the analysis of the key parameters of the IDW—its position and width—as a function of magnetostriction and microwire dimensions in order to demonstrate that its presence and size have significant effects, especially in microwires with nearly zero magnetostriction. An initial theoretical study of these parameters has been performed, followed by the experimental investigation of the IDW in order to check and validate the theoretical results. The theoretical study included the calculation of the width of the IDW in microwires with various compositions and dimensions of the metallic nucleus and of the glass coating by considering the balance between the magnetoelastic anisotropy energy and the exchange energy in the transition region in which preponderant internal stresses change from axial either to circumferential or radial. Then, we identified the cases in which calculations point to large values of the IDW's width and we performed experimental investigations on microwires with compositions and dimensions which are the closest to the theoretically predicted cases in which the effects of a rather thick IDW are expected to be observed. Experimental investigations include axial hysteresis loops, FMR, and GMI effect measurements. Axial hysteresis loops of amorphous microwires have been measured using a fluxmetric method. Microwave absorption FMR measurements were performed on amorphous microwires with the dc magnetic field applied parallel to their axes, employing a sample loaded, *X*-band waveguide. An Agilent E4991A impedance analyzer has been employed to perform the ultrahigh frequency GMI measurements up to a frequency of 3 GHz.

Calculated results show that the IDW has the largest width in nearly zero magnetostrictive microwires, in which the width exceeds or is similar to the thickness of the OS, and in which it produces the most visible effects. The results of the IDW study allow one to fully understand the domain structure and magnetic behavior of amorphous microwires and, at the same time, they offer a tool for tailoring their magnetic properties for targeted sensor applications.

## II. THEORETICAL CONSIDERATIONS AND RESULTS

In order to perform a theoretical analysis of the IDW between the IC and the OS, it is necessary to find the two key parameters that characterize it: its position and its width. The analysis of internal stresses induced during preparation is the basis for getting the necessary information on both these parameters.

Internal stresses have been calculated considering both stresses induced by the rapid solidification of metal and those induced by the difference between the thermal expansion coefficients of metal and glass. The glass transition phenomenon of the metal has been considered to be a simple solidification process, which, for simplicity, is assumed to take place simultaneously with the hardening of the actual glass coating at the glass transition temperature of the metallic alloy. The metallic nucleus has been considered as consisting of very thin successive concentric cylindrical shells which solidify consecutively starting from the outside. Therefore, stresses induced by rapid solidification have been calculated by solving the temperature field equation in cylindrical coordinates and then adding up the stresses induced by the solidification of the successive cylindrical shells as they progressively solidify. The contraction of two materials with different thermal expansion coefficients generates additional stresses following the solidification of metal and hardening of the glass coating. Consequently, stresses induced by the difference between the thermal expansion coefficients of metal and glass have been calculated by solving the equilibrium equation of the displacement vector of any point of the microwire, and then finding the components of the strain tensor and finally the induced stresses using Hooke's law. Since the nondiagonal components of the stress tensor are negligible compared to the diagonal ones, only the latter

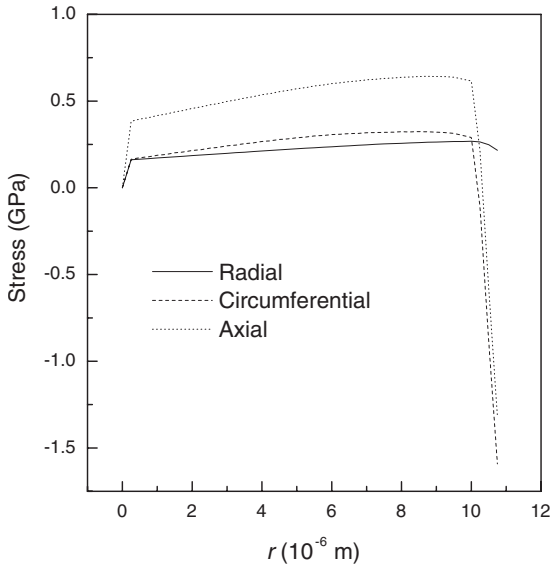


FIG. 1. Calculated radial distribution of internal stresses induced during preparation in a positive magnetostrictive $Fe_{77.5}Si_{7.5}B_{15}$ amorphous glass-coated microwire with $D_m=22$ $\mu$m and $t_g=5$ $\mu$m. The radial coordinate is denoted by $r$.

have been calculated—i.e., the axial ($\sigma_{zz}$), radial ($\sigma_{rr}$), and circumferential ($\sigma_{\theta\theta}$) ones. The mathematical formulation of both mechanisms responsible for the appearance of internal stresses in glass-coated microwires, together with the stress calculation method, is presented in a previous work.[7]

Figure 1 illustrates a typical radial distribution of the internal stresses induced during preparation in a positive magnetostrictive ($Fe_{77.5}Si_{7.5}B_{15}$) amorphous microwire. Given the tensor character of internal stresses, only the dominant components are important and they are the ones that determine the direction of the magnetoelastic anisotropy through the coupling with magnetostriction. In this case, for the $Fe_{77.5}Si_{7.5}B_{15}$ microwire with the diameter of the metallic core $D_m=22$ $\mu$m and the glass coating thickness $t_g=5$ $\mu$m, there are three regions of stress dominance on the radial direction: from the microwire's center ($r=0$) to the radial coordinate $r=10.15$ $\mu$m, the axial tensile stress dominates, followed by a very narrow region in which the radial tensile stress dominates (between $r=10.15$ $\mu$m and $r=10.30$ $\mu$m), and from this point toward the microwire's surface the compressive circumferential stress dominates. The three regions of stress dominance result only in two regions with different directions of the magnetoelastic anisotropy. The coupling between the dominant axial tensile stress and the positive magnetostriction results in a region with an axial direction of the magnetoelastic anisotropy from $r=0$ to $r=10.15$ $\mu$m. The coupling between the dominant radial tensile stress and the positive magnetostriction results in a region with a radial direction of anisotropy in the narrow region that follows, and finally, the coupling between the compressive circumferential stress and the positive magnetostriction results again in a zone with radial anisotropy in the remaining region toward the surface of the microwire. Consequently, from the point of view of the magnetoelastic anisotropy, there are only two distinct regions: one with axial and another one with radial anisotropy axis. The exact separation coordinate on the radial direction is $r=10.15$ $\mu$m. Therefore, one can associate this coordinate with the middle of the IDW. Thus, the first of the two key parameters of the IDW is known. In a similar way, starting from the radial distribution of internal stresses, one can find the position of the IDW in amorphous microwires with any dimensions and with various compositions.

The width of the IDW, $\delta$, is given by[20]

$$\delta=\sqrt{C/2K}, \tag{1}$$

where $C$ is the exchange constant and $K$ the magnetoelastic anisotropy constant. For Fe based alloys $C=2\times10^{-11}$ J m$^{-1}$, while for Co based ones $C=3\times10^{-11}$ J m$^{-1}$.

The magnetoelastic anisotropy constant $K$ is given by

$$K=(3/2)\lambda_S\langle\sigma\rangle, \tag{2}$$

where $\langle\sigma\rangle$ is the average value of the internal stresses across the transition region in which the direction of the dominant stress changes. In order to calculate the value of $\langle\sigma\rangle$, we performed a detailed analysis of the internal stresses in the transition region. The results of the analysis show that there are cases in which axial tensile stresses change through the wall to radial tensile ones as in the case illustrated in Fig. 1, as well as cases in which axial tensile stresses change directly to compressive circumferential ones, without going through an intermediate zone with radial tensile stresses. We will go back to the detailed results of this analysis later, when we will discuss the dependence of the IDW width on the physical dimensions of microwires.

Hence, based on the radial distribution of internal stresses, one can calculate the second of the two key parameters of the IDW, i.e., its width.

The width of the IDW in the case of the $Fe_{77.5}Si_{7.5}B_{15}$ microwire with $D_m=7$ $\mu$m and $t_g=5$ $\mu$m is 14.1 nm, while for a microwire with the same composition and glass coating thickness, but $D_m=25$ $\mu$m, the width of the IDW is 26 nm. For $Co_{68.15}Fe_{4.35}Si_{12.5}B_{15}$ microwires with the same dimensions, $\delta$ is 273 nm (for $D_m=7$ $\mu$m) and over 500 nm (for $D_m=25$ $\mu$m), respectively. Meanwhile, $\delta$ for $Co_{80}Si_{10}B_{10}$ microwires is between 70 and 100 nm. These results show that magnetostriction influences in the most significant way the width of the IDW. Thus, microwires with large and positive magnetostriction ($\lambda_S>0$) display the thinnest IDW, with $\delta$ ranging between 10 and 30 nm. Negative magnetostrictive microwires ($\lambda_S<0$), such as $Co_{80}Si_{10}B_{10}$ ones, display intermediate values of $\delta$ (between 70 and 100 nm), while nearly zero magnetostrictive ones ($\lambda_S\approx0$), e.g., $Co_{68.15}Fe_{4.35}Si_{12.5}B_{15}$ ones, display the largest values for the width of the IDW. These observations could serve as a basis to disregard in some degree the effects of the IDW in microwires with highly positive or negative magnetostriction. Nevertheless, in the case of nearly zero magnetostrictive microwires, one has to take into account the IDW due to its large width, which is expected to produce experimentally visible effects.

Given the various compositions of microwires, the wide range of values for the diameter of their metallic nucleus, as well as the wide range of values for their glass coating thick-

TABLE I. Calculated values of the IDW width ($\delta$), OS thickness ($t_{OS}$), and IC diameter ($D_{IC}$) for $Co_{68.15}Fe_{4.35}Si_{12.5}B_{15}$ microwires with $D_m$=22 $\mu$m and $t_g$ ranging between 2 and 30 $\mu$m.

| $t_g$ ($\mu$m) | $\delta$ (nm) | $t_{OS}$ (nm) | $D_{IC}$ ($\mu$m) |
|---|---|---|---|
| 2 | 652 | 224.0 | 20.248 |
| 3 | 648 | 126.0 | 20.452 |
| 4 | 560 | 570.0 | 19.740 |
| 5 | 529 | 585.5 | 19.771 |
| 6 | 505 | 597.5 | 19.795 |
| 7 | 566 | 467.0 | 19.934 |
| 8 | 552 | 474.0 | 19.948 |
| 9 | 533 | 483.5 | 19.967 |
| 10 | 518 | 491.0 | 19.982 |
| 15 | 472 | 514.0 | 20.028 |
| 20 | 450 | 525.0 | 20.050 |
| 25 | 472 | 414.0 | 20.228 |
| 30 | 466 | 417.0 | 20.234 |

ness, and since at this time only the cases in which $\delta$ is as large as possible are of interest, we will focus in the following on microwires in which the widest IDWs are expected, i.e., those with nearly zero magnetostriction, such as the $Co_{68.15}Fe_{4.35}Si_{12.5}B_{15}$ ones. For microwires with this composition, an optimum value for the diameter of their metallic nucleus, $D_m$, will be selected, and then the dependence of $\delta$ on their glass coating thickness, $t_g$, will be investigated. Based on very recent results on the optimization of the GMI response of Co-based amorphous microwires,[18] we have chosen $D_m$=22 $\mu$m, since around this value of the diameter of the metallic nucleus the magnetoelastic anisotropy constant near the microwire surface reaches the minimum value, and according to Eq. (1) the largest width of the IDW is expected.

Calculated values of the IDW width, $\delta$, for $Co_{68.15}Fe_{4.35}Si_{12.5}B_{15}$ microwires with $D_m$=22 $\mu$m and $t_g$ ranging from 2 to 30 $\mu$m are listed in Table I. The case of $t_g$=1 $\mu$m has not been included, as the preparation of microwires with such thin glass coating is difficult due to reproducibility issues and it would be rather complicated to verify experimentally the results of the calculations in this particular case.

Figure 2 shows the dependence of $\delta$ on $t_g$ for $Co_{68.15}Fe_{4.35}Si_{12.5}B_{15}$ microwires with $D_m$=22 $\mu$m as it results from Table I. One observes a maximum that appears between $t_g$=6 $\mu$m and $t_g$=10 $\mu$m, which interrupts the monotonic decrease of the IDW width with the thickness of the glass coating.

In order to find the origins of this maximum, we had to go back to the detailed analysis of the internal stresses in the region of the wall and to check in each case the sign and orientation of stresses on each side of the IDW.

For 2 $\mu$m$\leqslant t_g \leqslant$6 $\mu$m, the axial tensile stress ($\sigma_{zz}>0$) changes to radial tensile stress ($\sigma_{rr}>0$) through this region. For instance, Fig. 3 illustrates the stresses within the transition region of a microwire with $D_m$=22 $\mu$m and $t_g$=4 $\mu$m. The dark area represents stresses induced due to the difference in the thermal expansion coefficients of metal and glass, while the light area represents the stresses induced due to rapid solidification. The situation is similar for the microwires with $t_g$ of 2, 3, 5, and 6 $\mu$m. The maximum values of both $\sigma_{zz}$ and $\sigma_{rr}$ increase with $t_g$, and the ratio between stresses induced by rapid solidification and those induced by the difference between thermal expansion coefficients varies from case to case. Nevertheless, this ratio does not appear to be important in this range of values of $t_g$. Also, all the stresses in this range are positive (tensile).

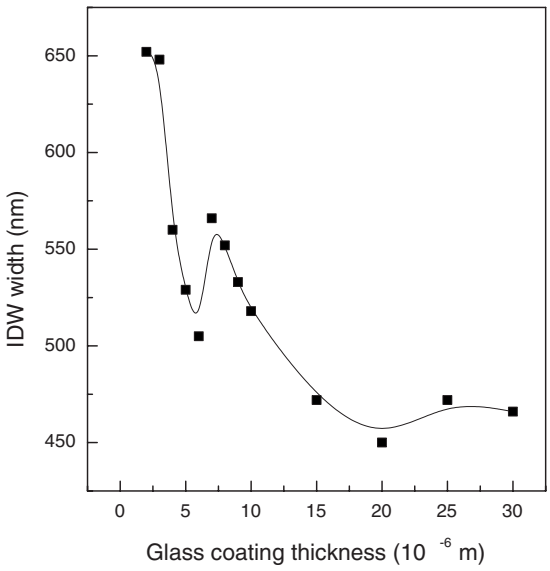


FIG. 2. Dependence of the IDW width, $\delta$, on the thickness of the glass coating, $t_g$, for $Co_{68.15}Fe_{4.35}Si_{12.5}B_{15}$ amorphous glass-coated microwires with $D_m$=22 $\mu$m.

The situation changes significantly at $t_g$=7 $\mu$m (see Fig. 4). First of all, the axial tensile stress ($\sigma_{zz}>0$) changes to circumferential compressive stress ($\sigma_{\theta\theta}<0$) when going

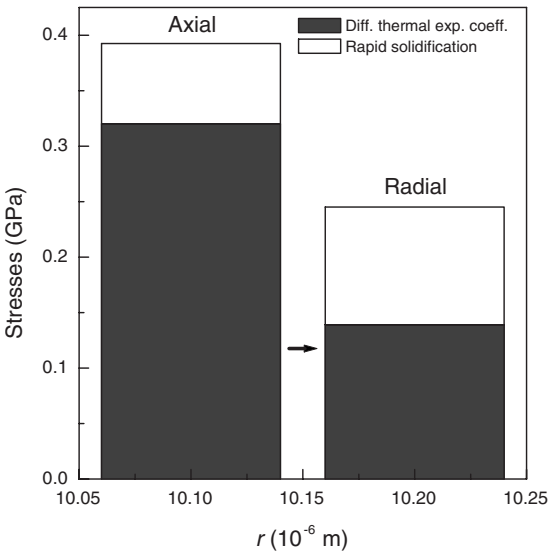


FIG. 3. Internal stresses in the transition region of a $Co_{68.15}Fe_{4.35}Si_{12.5}B_{15}$ amorphous glass-coated microwire with $D_m$=22 $\mu$m and $t_g$=4 $\mu$m.

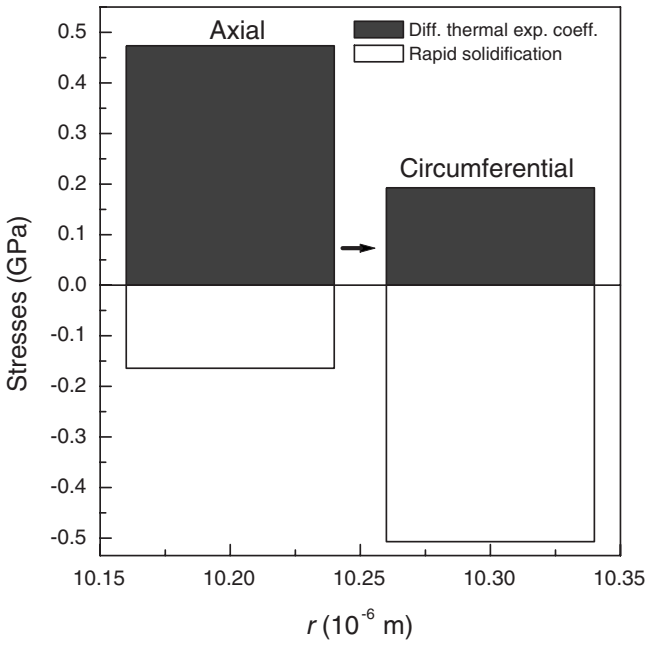


FIG. 4. Internal stresses in the transition region of a $Co_{68.15}Fe_{4.35}Si_{12.5}B_{15}$ amorphous glass-coated microwire with $D_m = 22\ \mu m$ and $t_g = 7\ \mu m$.

through the region of the wall. One observes that stresses induced by rapid solidification are negative (compressive) for both $\sigma_{zz}$ and $\sigma_{\theta\theta}$, in spite of the fact that the total axial stress is positive.

For $8\ \mu m \leqslant t_g \leqslant 20\ \mu m$, again the axial tensile stress changes to radial tensile stress through the wall, similar to the first case, for the thinner glass coating. However, there is a difference as compared to the range $2-6\ \mu m$, namely, that the part of the axial stress induced by rapid solidification remains negative (compressive). For $t_g > 20\ \mu m$, the axial tensile stress changes to circumferential compressive stress through the region of the wall, and the rapid solidification part is always negative, similar to the case of the $7\ \mu m$ glass coating, but with larger values of the stresses.

Summarizing, the nonlinear dependence of $\delta$ on $t_g$ originates in the nonlinear dependence of internal stresses induced during preparation on the same parameter. More specifically, the nonlinearity arises from the change of stress orientation when going through the region of the wall, and on the sign and magnitude of the individual stress components, i.e., those induced by the difference between the thermal expansion coefficients of metal and glass and those induced by the rapid solidification of the metal. Essentially, the thickness of the glass coating is affecting in a nonlinear way both processes responsible for the appearance of internal stresses during the preparation of the microwire: rapid solidification of metal and thermal shrinking of the metal-glass composite. The dependence of a magnetic parameter, such as the width of the IDW, on the dimensions of microwires, reveals the critical importance of the technological parameters employed in the microwire preparation process (e.g., temperature of the molten alloy, ejection pressure, etc.) in establishing, via the two mechanisms responsible for the appearance of internal stresses, the magnetic properties of the amorphous glass-coated microwires.

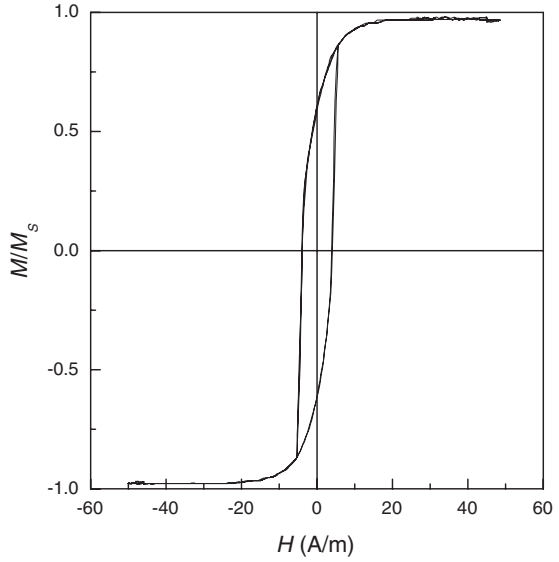


FIG. 5. Low field axial hysteresis loop of a $Co_{68.15}Fe_{4.35}Si_{12.5}B_{15}$ amorphous glass-coated microwire with $D_m = 22\ \mu m$ and $t_g = 2.05\ \mu m$.

## III. EXPERIMENTAL EVIDENCE AND DISCUSSION

Let us investigate the experimental data providing the proof for the existence of wide IDWs in $Co_{68.15}Fe_{4.35}Si_{12.5}B_{15}$ amorphous glass-coated microwires with $D_m = 22\ \mu m$ and various values of $t_g$. Amorphous glass-coated microwires with the metallic nucleus diameter of $22\ \mu m$ and various values of the glass coating thickness between 2 and $30\ \mu m$ have been prepared by the glass-coated melt spinning technique at the National Institute of R&D for Technical Physics, Iaşi, Romania.

Calculations predict the widest IDW for $t_g = 2$ and $t_g = 3\ \mu m$, respectively. Since $D_m > 20\ \mu m$, a square low field axial hysteresis loop is expected, typical for the presence of the LBE. The LBE appears as a result of the one step magnetization reversal within the axially magnetized IC. As the applied field is slightly increased, one should see the effects of the wide IDW as well as of the much thinner OS in both cases (see Table I). Despite the very thin OS (224 nm for $t_g = 2\ \mu m$ and 126 nm for $t_g = 3\ \mu m$, respectively), complete saturation of the microwires would be rather difficult to reach due to the very large transverse magnetoelastic anisotropy of the OS, determined by the very large circumferential stresses which increase abruptly toward the surface of the microwire's metallic nucleus (see, for instance, Fig. 1).

Figures 5 and 6 show the low field axial hysteresis loops of two microwires with the diameter of the metallic nucleus of $22\ \mu m$ and glass coating thicknesses of 2.05 and $2.85\ \mu m$, respectively. As the applied field is reduced from its maximum value, there is a first region in which the magnetization rotates slowly from the axial direction. This region is attributed to the thin OS with large circumferential aniso-

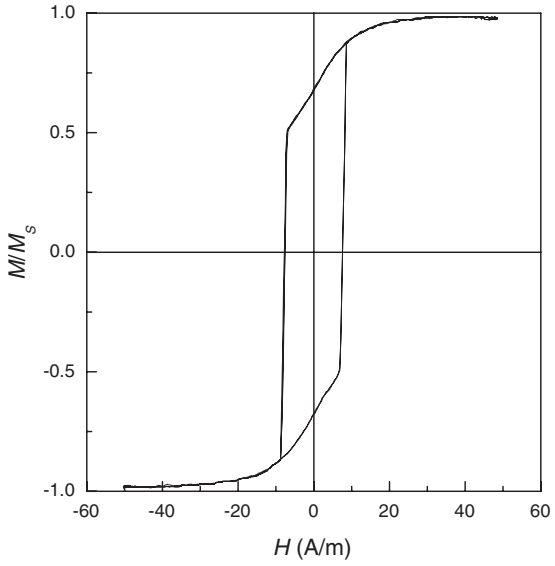


FIG. 6. Low field axial hysteresis loop of a $Co_{68.15}Fe_{4.35}Si_{12.5}B_{15}$ amorphous glass-coated microwire with $D_m$ =22 $\mu$m and $t_g$=2.85 $\mu$m.

tropy. Further decrease of the field results in a much quicker decrease of the magnetization, corresponding to a region with small average anisotropy, attributed to the wide IDW. The third region is in both cases the one step reversal of magnetization in the IC. The three regions of the domain structure are also clearly visible in microwires with thicker glass coating, either in cases in which $\delta$ is expected to be larger than $t_{OS}$ (e.g., for a microwire with $t_g$=6.57 $\mu$m—Fig. 7), or in cases in which $\delta$ is expected to be smaller than $t_{OS}$ (e.g., Fig. 8 illustrates the hysteresis loop of a microwire with $t_g$=4.25 $\mu$m). For comparison, Fig. 9 shows the low field axial hysteresis loop in case of an $Fe_{77.5}Si_{7.5}B_{15}$ amorphous glass-coated microwire with $D_m$=23 $\mu$m and $t_g$ =9.5 $\mu$m. The width of the IDW in this case is less than 20 nm and the thickness of the OS is below 200 nm. Therefore, one can see only the one step reversal of the magnetization from the IC. Thus, axial hysteresis loops prove the existence of wide IDWs in $Co_{68.15}Fe_{4.35}Si_{12.5}B_{15}$ amorphous glass-coated microwires and confirm the existence of very narrow IDWs in highly magnetostrictive amorphous microwires.

One would expect a relation between the remanence to saturation ratio ($M_R/M_S$) on one hand, and the ratio between the volume of the IC and that of the metallic nucleus on the other hand, similar to that used in Ref. 21. Nevertheless,

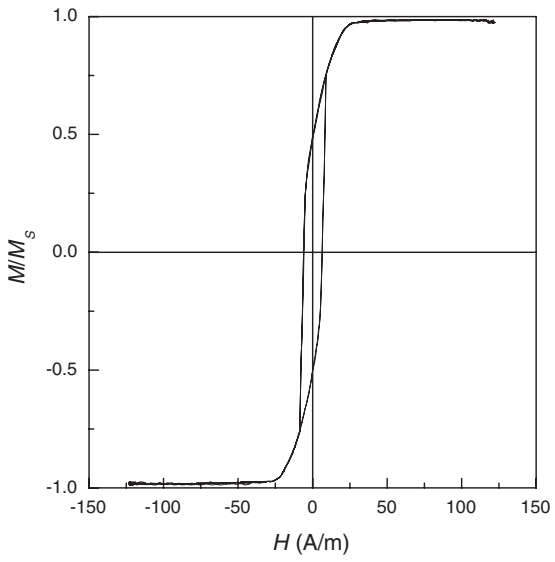


FIG. 7. Low field axial hysteresis loop of a $Co_{68.15}Fe_{4.35}Si_{12.5}B_{15}$ amorphous glass-coated microwire with $D_m$ =22 $\mu$m and $t_g$=6.57 $\mu$m.

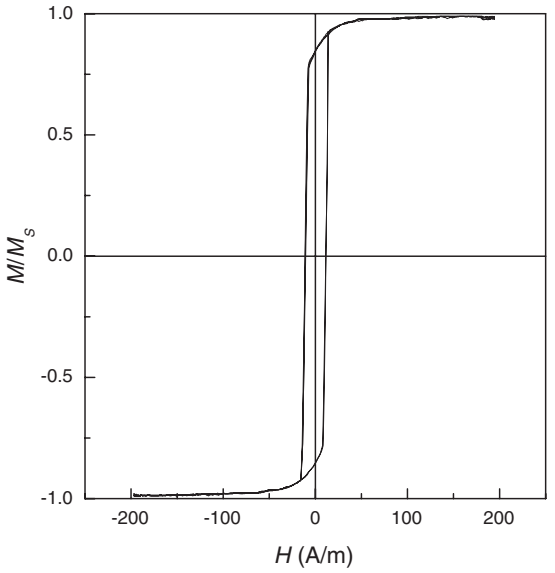


FIG. 8. Low field axial hysteresis loop of a $Co_{68.15}Fe_{4.35}Si_{12.5}B_{15}$ amorphous glass-coated microwire with $D_m$ =22 $\mu$m and $t_g$=4.25 $\mu$m.

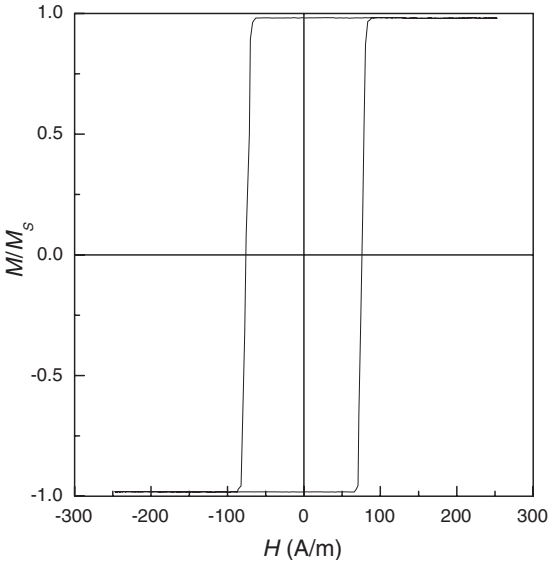


FIG. 9. Low field axial hysteresis loop of an $Fe_{77.5}Si_{7.5}B_{15}$ amorphous glass-coated microwire with $D_m$=23 $\mu$m and $t_g$ =9.5 $\mu$m.

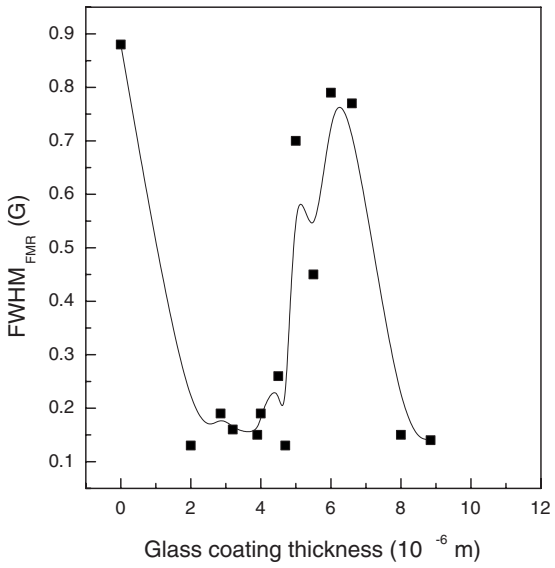


FIG. 10. Dependence of the FMR linewidth $\Delta B$ ($FWHM_{FMR}$) of $Co_{68.15}Fe_{4.35}Si_{12.5}B_{15}$ amorphous glass-coated microwires with $D_m = 22$ $\mu$m on the glass coating thickness for a resonance frequency of 9.5 GHz.

such a relation has been always employed in case of highly magnetostrictive amorphous microwires in which $\delta$ is almost negligible, as it has been pointed out in the previous section and proved in this section. This relation, which is reduced to $M_R/M_S=(D_{IC}/D_m)^2$, is no longer valid in case of wide IDWs, such as the case of $Co_{68.15}Fe_{4.35}Si_{12.5}B_{15}$ bistable microwires. Moreover, this is exactly a consequence of the existence of IDWs with large values of $\delta$.

Since IDWs are rather close to the surface of the metallic nucleus, another technique chosen to experimentally investigate their presence and width is FMR. Special attention has been paid to microwires with the glass coating thickness up to 10 $\mu$m in order to check the appearance of the theoretically predicted maximum in the dependence of $\delta$ on $t_g$.

Figure 10 shows the dependence of the FMR linewidth $\Delta B$, defined as the full width at half maximum of the resonance curves ($FWHM_{FMR}$), on the glass coating thickness for a resonance frequency of 9.5 GHz. Since $\Delta B$ is proportional to the degree in which local anisotropies are spread,[22] it is also an indication of the IDW width, as the highest degree of spread is encountered within the wall. Despite the rather scattered results depicted in Fig. 10, one can clearly see the maximum that appears at values of $t_g$ around 6–7 $\mu$m, maximum that corresponds to that displayed by the dependence of $\delta$ on $t_g$ (see Fig. 2). The largest value of $\Delta B$ is obtained for a sample with the glass coating completely removed ($t_g=0$) with a solution of hydrofluoric acid.[21] The values of $\Delta B$ are smaller than expected for $t_g$ between 2 and 3 $\mu$m. A plausible explanation is that in this case the penetration depth of the microwave field exceeds the OS and the IDW, reaching into the IC with highly ordered magnetic moments and large axial anisotropy. Because of this, the spread of local anisotropies within the wall is masked by the clearly defined anisotropy of the IC. For the sample with the glass coating removed, the wall is much wider and the microwave field does not reach into the IC. This case has not been calculated since the microwire with removed glass coating is not an as-cast sample, and the distribution of internal stresses cannot be calculated as described in the previous section. For microwires with $t_g$ between 5 and 10 $\mu$m the depth of the region formed by the OS and the IDW is larger than in the case of microwires with $t_g$ between 2 and 3 $\mu$m (see Table I) and again the microwave field does not reach into the highly ordered IC. As a consequence, the FMR signal proportional to the wall width is clearly observed. Hence, the nonlinear dependence of $\delta$ on $t_g$ has been confirmed by means of FMR measurements, despite some inadvertencies generated by the impossibility to match exactly the FMR frequency to have only the FMR response of the interdomain wall. The response of the OS cannot be avoided, being the top layer of the microwire's magnetic domain structure, and in some cases, the responding region includes even a small part of the IC.

The measurement of the GMI effect is another technique that allows the investigation of a shell located toward the surface of the microwire's metallic nucleus. In this case, the working frequency can be reduced as compared to that employed in FMR measurements in order to study a thicker layer of the substance. Again, the GMI linewidth ($\Delta B_{GMI}$), defined as the FWHM of the GMI curves ($FWHM_{GMI}$), is the parameter that offers, among other information, the most valuable information about the width of the IDW, due to the same reasons as in the case of FMR. After analyzing the GMI spectra of many samples with various values of the glass coating thickness, the conclusion was that the values of $\Delta B_{GMI}$ extracted from the spectra obtained at 1.5 GHz follow most accurately the calculated width of the IDW. Finding the optimum frequency was again, similar to the case of FMR, a question of correlation between the penetration depth of the ac driving current on one hand, and the thickness of the OS, the width of the IDW, and the diameter of the IC on the other. Figure 11 shows the dependence of $\Delta B_{GMI}$ that corresponds to 1.5 GHz on $t_g$ for microwires with $D_m=22$ $\mu$m. One observes that the general trend of the curve that gives the experimental dependence of $\Delta B_{GMI}$ on $t_g$ is similar to the one which gives the theoretical dependence of $\delta$ on $t_g$. The values of $\Delta B_{GMI}$ for $t_g$ of 2 and 3 $\mu$m are large and there is clear evidence of a maximum between $t_g=5$ $\mu$m and $t_g=10$ $\mu$m. It is easier to detect the wide IDW for $t_g$ of 2 or 3 $\mu$m in GMI measurements as compared to FMR ones, since the GMI response of a sample is much more sensitive to the smallest anisotropy of the region in which skin effect occurs, given that the existence of very good soft magnetic properties is one of the basic criteria to obtain a sensitive GMI effect. As a result, GMI effect measurements substantiate the theoretical results on the wide IDWs in $Co_{68.15}Fe_{4.35}Si_{12.5}B_{15}$ amorphous glass-coated microwires, and especially the nonlinear dependence of the wall width on the thickness of the glass coating.

Summarizing, hysteresis loops together with FMR and GMI measurements offer a comprehensive picture of the domain structure in $Co_{68.15}Fe_{4.35}Si_{12.5}B_{15}$ amorphous glass-coated microwires, and confirm the calculated results on the IDW and its width in these materials.

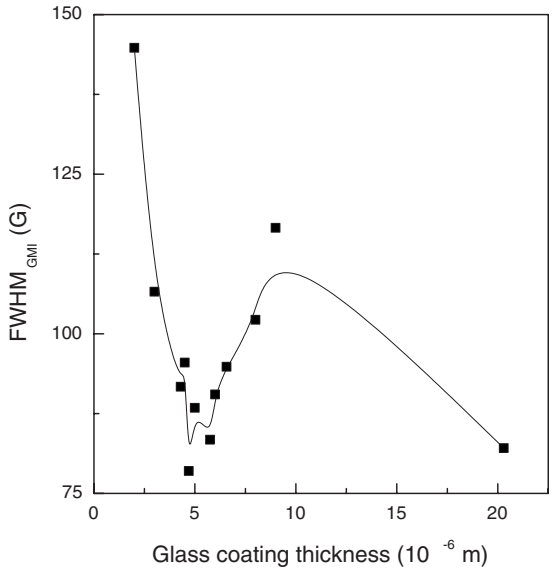


FIG. 11. Dependence of the GMI linewidth $\Delta B_{GMI}$ (FWHM$_{GMI}$) of $Co_{68.15}Fe_{4.35}Si_{12.5}B_{15}$ amorphous glass-coated microwires with $D_m$=22 $\mu$m on the glass coating thickness for a frequency of the ac driving current of 1.5 GHz.

## IV. CONCLUSIONS

The width of the IDW between the inner core and outer shell of amorphous glass-coated microwires has been investigated.

Calculations have shown that the largest width of the IDW—over 650 nm—is displayed by amorphous microwires with nearly zero magnetostriction. Amorphous microwires with large positive magnetostriction and those with negative magnetostriction display IDWs of a few tens of nanometers, maximum of 100 nm. The dependence of the wall width on glass coating thickness is nonlinear, displaying a maximum between 5 and 10 $\mu$m of glass thickness. The appearance of this maximum originates in the nonlinear dependence of internal stresses induced during preparation on the thickness of the glass coating.

The presence of wide IDWs in nearly zero magnetostrictive microwires is confirmed by axial hysteresis loop measurements. The nonlinear dependence of the IDW width on the thickness of the glass coating is confirmed by means of FMR and GMI effect measurements.

Given that the wide IDW in nearly zero magnetostrictive amorphous microwires is located close to the microwire surface, the dependence of its width on microwire dimensions offers a tool for tailoring the magnetic properties of such microwires, especially for magnetic sensors designed for high frequency applications, e.g., those operating on the principle of the GMI effect—knowing the sensitive correlation between the GMI response and the existence of very good soft magnetic properties in the surface region of microwires.

The results of the experimental and theoretical investigation of the IDW in amorphous glass-coated microwires are of interest for understanding their basic magnetic properties and behavior, e.g., their axial and circumferential quasistatic and dynamic hysteresis loops and the dependence of their permeability on the frequency of the applied magnetic field.

Future work will aim to demonstrate the ways in which the rigorous control of the IDW width can be employed to improve the GMI response of nearly zero magnetostrictive amorphous glass-coated microwires.

[1] D. C. Jiles, Acta Mater. **51**, 5907 (2003).
[2] R. Hasegawa, J. Non-Cryst. Solids **329**, 1 (2003).
[3] M. Vázquez and A. Hernando, J. Phys. D **29**, 939 (1996).
[4] M. Vázquez, Physica B **299**, 302 (2001).
[5] K. Mohri, T. Uchiyama, L. P. Shen, C. M. Cai, L. V. Panina, Y. Honkura, and M. Yamamoto, IEEE Trans. Magn. **38**, 3063 (2002).
[6] H. Chiriac and T.-A. Óvári, Prog. Mater. Sci. **40**, 333 (1996).
[7] H. Chiriac, T.-A. Óvári, and Gh. Pop, Phys. Rev. B **52**, 10104 (1995).
[8] A. S. Antonov, V. T. Borisov, O. V. Borisov, A. F. Prokoshin, and N. A. Usov, J. Phys. D **33**, 1161 (2000).
[9] R. Varga, K. L. Gracía, M. Vázquez, A. Zhukov, and P. Vojtanik, Phys. Rev. B **70**, 024402 (2004).
[10] A. Zhukov, V. Zhukova, J. M. Blanco, A. F. Cobeño, M. Vázquez, and J. González, J. Magn. Magn. Mater. **258-259**, 151 (2003).
[11] H. Chiriac, S. Corodeanu, M. Ţibu, and T.-A. Óvári, J. Appl. Phys. **101**, 09N116 (2007).
[12] H. Chiriac, J. Yamasaki, T.-A. Óvári, and M. Takajo, IEEE Trans. Magn. **35**, 3901 (1999).
[13] Yu. Kabanov, A. Zhukov, V. Zhukova, and J. González, Appl. Phys. Lett. **87**, 142507 (2005).
[14] J. Velázquez, M. Vázquez, and A. P. Zhukov, J. Mater. Res. **11**, 2499 (1996).
[15] S. Puerta, D. Cortina, H. García-Miquel, D.-X. Chen, and M. Vázquez, J. Non-Cryst. Solids **287**, 370 (2001).
[16] R. Varga, K. L. García, M. Vázquez, and P. Vojtanik, Phys. Rev. Lett. **94**, 017201 (2005).
[17] H. Chiriac and T.-A. Óvári, IEEE Trans. Magn. **38**, 3057 (2004).
[18] H. Chiriac, S. Corodeanu, M. Ţibu, and T.-A. Óvári, IEEE Trans. Magn. **43**, 2977 (2007).
[19] A. Chizhik, J. M. Blanco, A. Zhukov, J. Gonzalez, C. Garcia, P. Gawronski, and K. Kulakowski, IEEE Trans. Magn. **42**, 3889 (2006).
[20] A. Aharoni, *Introduction to the Theory of Ferromagnetism* (Clarendon, Oxford, 1998), p. 140.
[21] H. Chiriac, Gh. Pop, F. Bararіu, and M. Vázquez, J. Appl. Phys. **75**, 6949 (1994).
[22] F. M. Tufescu, H. Chiriac, T.-A. Óvári, and A. Stancu, J. Magn. Magn. Mater. **242-245**, 254 (2002).